Diagnostic Pathology

BRIEF REPORT Open Access

EWSR1::BEND2 fusion sarcoma of the urinary bladder – a case report and review of literature

Vili Halava[1], Jenni Tuominen[2], Paula Lindholm[3], Timo Kyyrönen[4], Markku Kallajoki[1] and Katri Orte[1*]

Abstract

In this case report we describe a Ewing-like high grade small round cell sarcoma of the urinary bladder in which an extremely rare *EWSR1::BEND2* fusion was found. A 28-year-old male patient presented with hematuria and in the following examinations a large necrotic bladder tumor with spreading to adjacent prostatic tissue and multiple lung metastases were found. Histology showed a poorly differentiated small round cell tumor with perivascular rosettes and moderate membranous positivity for CD99. The methylation profile of the tumor did not match with any of the tumor entities grouped by the sarcoma classifier. With tumor agnostic methods, mainly next generation sequencing, novel fusions are being found at an accelerating rate. Our case adds to the expanding group of EWSR1 fusion neoplasms, and describes the effects of a Ewing sarcoma treatment protocol on this type of sarcoma. The relevance of traditional methods for detecting Ewing sarcoma with fluorescence in situ hybridization is decreasing as *EWSR1* rearrangements are detected in tumors that show different clinical behavior and morphology. The classification of these tumors into WHO defined entities to guide treatment is a challenge.

Keywords Fusion sarcoma, EWSR1:BEND2, Undifferentiated small round cell sarcoma, Ewing-like sarcoma

Background

Next generation sequencing (NGS) now enables large scale random genetic testing in routine diagnostics, marking a new era for sarcoma diagnostics. Earlier methods, such as real-time polymerase chain reaction (RT-PCR) or fluorescence in situ hybridization (FISH), focused on detecting single genetic alterations. These have been replaced by genome-wide search to reveal distinct driver mutations even in ultra-rare sarcomas. As a result, the undifferentiated small round cell sarcoma group has dispersed into smaller tumor groups of a few or even single patients.

The treatment strategy in such cases is difficult to define, since data from larger cohorts are not available. Accurate, up-to-date molecular diagnostics are therefore essential both for guiding treatment strategies and improving prognosis prediction of these ultra-rare tumor types.

Here, we describe a case of *EWSR1::BEND2* fusion sarcoma of the bladder in a previously healthy male. At diagnosis, the tumor was classified as extraskeletal Ewing sarcoma, and the therapy followed standard Ewing sarcoma protocols. Only later, as a part of a validation

*Correspondence:
Katri Orte
katri.orte@tyks.fi
[1]Department of Pathology, TYKS Laboratories, Turku University Hospital and University of Turku, Turku, Finland
[2]Laboratory of Molecular Haematology and Pathology, Department of Genomics, TYKS Laboratories, Turku University Hospital and University of Turku, Turku, Finland
[3]Department of Oncology, Turku University Hospital and University of Turku, Turku, Finland
[4]Department of Radiology, Turku University Hospital and University of Turku, Turku, Finland

cohort, RNA sequencing revealed the *EWSR1::BEND2* fusion. We discuss this finding in the context of literature and its implications for tumor classification.

Case presentation

A previously healthy 28-year-old obese male presented with haematuria. In cystoscopy, an exophytic 2 cm tumor with necrotic surface was detected near the orifice of the left ureter and the patient was referred to university hospital for further diagnostics and treatment.

Contrast enhanced CT-scan showed 4.5 cm lobular tumor at the bottom of the bladder and the left wall of the bladder was thickened (Fig. 1A, arrow heads). The border to the perivesical tissue was indefinite and the calcified tumor tissue spread parailiacally and infiltrated the lesser pelvis. The parailiacal lymph nodes on the left side were enlarged, and the left ureter was dilatated. A whole-body CT scan showed multiple pulmonary metastases (Fig. 1B) and there was decrease in contrast enhancement of large veins suggesting deep vein thrombosis. A bone scintigraphy showed no signs of bone involvement.

Transurethral tumor resection was performed. Nearly the entire left side of the bladder was covered in necrotic tissue that extended to the orifice of the ureter and the bottom of the bladder. The prostate was also abnormal and suspicious for malignancy. On a whole, the tumor seemed inoperable. Resection material consisted of a diffusely growing small blue round cell tumor with scanty clear cytoplasm with some cytoplasmic eosinophilic globules (Fig. 2A). Small and round nuclei had tightly packed chromatin and distinguishable nucleoli. Tumor cells formed rosette-like structure surrounding small vessels (Fig. 2B) but no other secondary structures were seen. Mitotic rate was 15/10HPF and small areas of necrosis were seen. Tumor tissue grew into contact with the bladder epithelium, showing mature squamous metaplasia (Fig. 2C, asterisk). The tumor tissue also infiltrated benign prostatic glands in the prostatic biopsy. The tumor cells were diffusely membrane positive for CD99 (Fig. 3A) and positive for EMA (Fig. 3B). Proliferation with Ki-67 staining was high, 70%. Cytoplasmic perinuclear spotted golgi-like staining pattern of low molecular weight cytokeratin (Cam 5.2 antibody) and vimentin, with greater intensity, were seen (Fig. 3C-D). Other cytokeratin stains (cytokeratin 7, cytokeratin 20 and high molecular weight keratin) were negative. Lymphatic markers (CD45, CD20 and CD3), germ cell markers (c-KIT, CD30, PLAP and hCG), neuroendocrine markers (synaptophysin and chromogranin A) and variety of other stains (panmelanocytic marker, desmin, myogenin, WT-1, CD34, PSA, PAS and AB-PAS) were negative. INI1 and SMARCA4 were retained. *EWSR1* fluorescence in situ hybridization showed a translocation in majority of the cells (Fig. 4A). Taken together, diagnosis of an

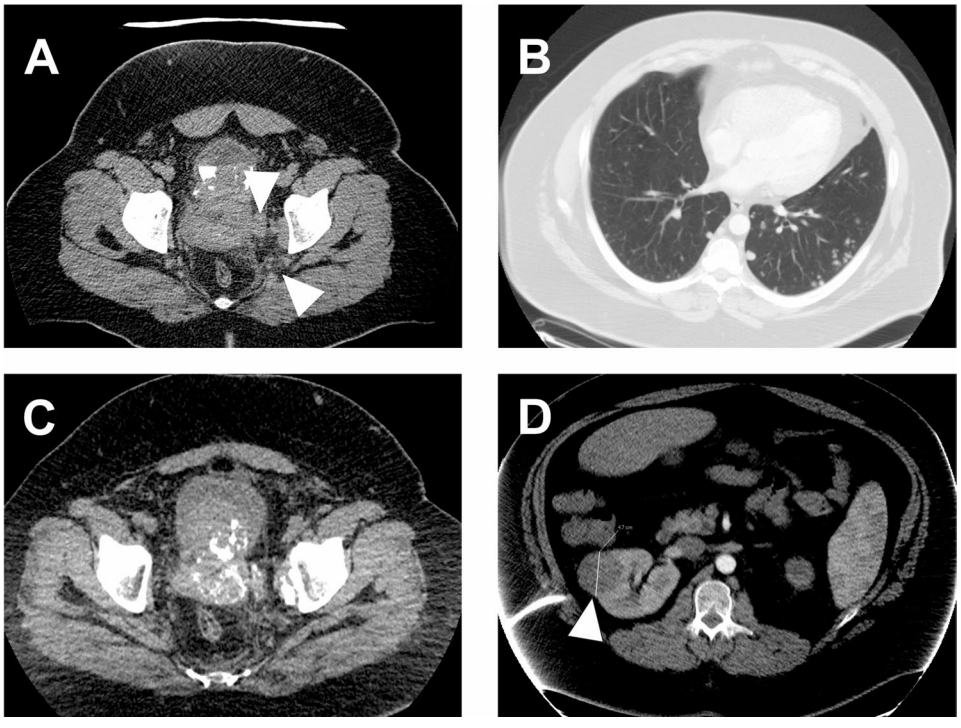

Fig. 1 CT scans of the abdomen and body. A large tumor mass behind the bladder at the time of diagnosis (**A**, arrow heads). Multiple pulmonary metastases 1 month after diagnosis (**B**). Progression of the calcified tumor 26 months after diagnosis (**C**). Metastatic tumor mass of the right kidney marked by arrow head, approx. 4.7 cm in diameter, 23 months after diagnosis (**D**)

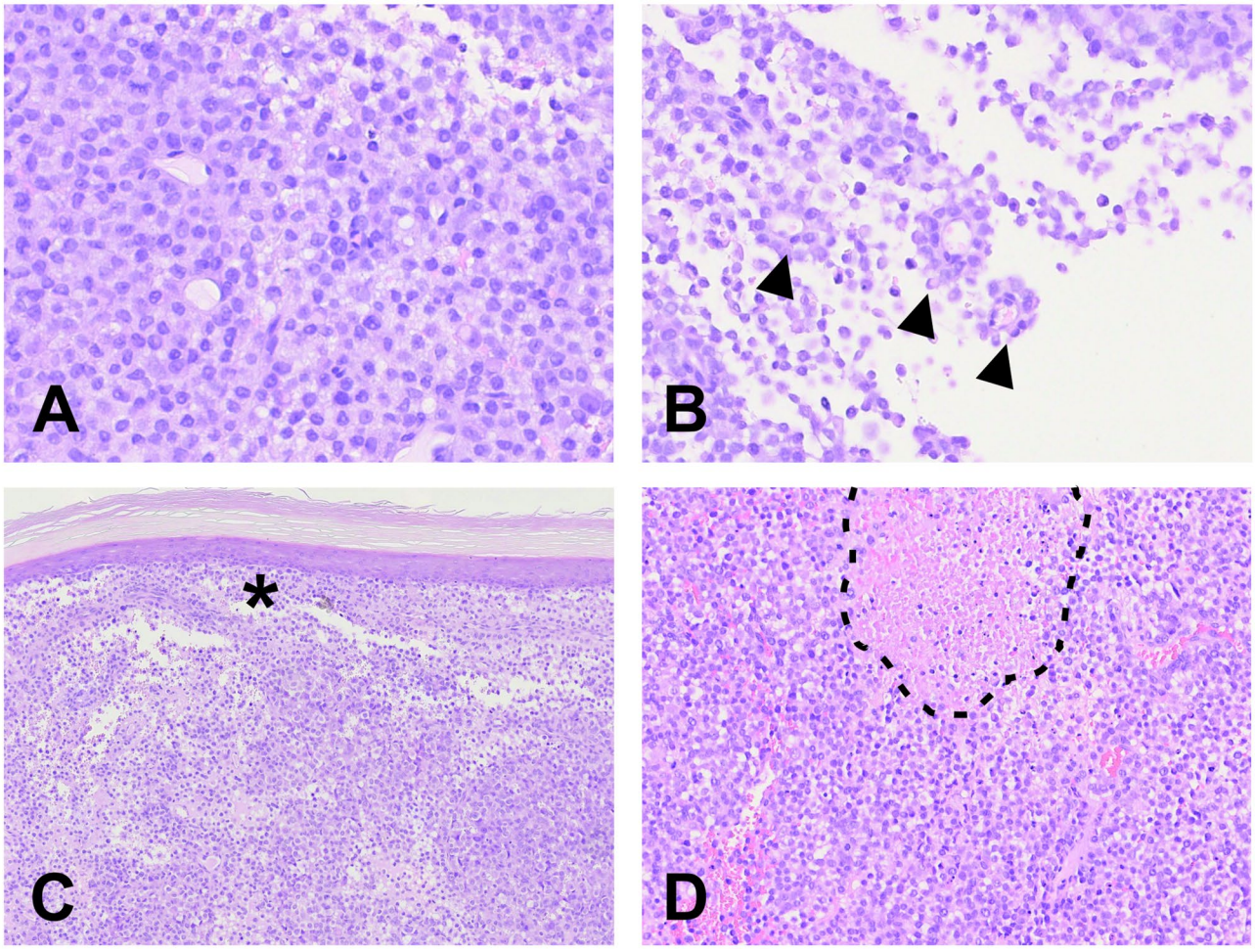

Fig. 2 Diffusely growing small blue round cell tumor with scanty clear cytoplasm and cytoplasmic eosinophilic globules (**A**, 40x). Tumor cells surrounding small vessels by forming a rosette-like structure, marked by arrowheads (**B**, 40x). Mature squamous metaplasia with tumor tissue growing into contact with the bladder epithelium, marked by asterisk (**C**, 20x). Necrotic tissue marked by dotted line (**D**, 20x)

extraskeletal Ewing sarcoma of the bladder with spread to adjacent prostate, was made.

After Ewing sarcoma diagnosis, doxorubicin neoadjuvant monotherapy was changed to ISG/SSG IV (Italian-Scandinavian Sarcoma Group IV) treatment protocol for Ewing family of tumours, consisting of vincristine, doxorubicin, ifosfamide and etoposide in different combinations [1]. During chemotherapy, the patient had persisting dysuria, pollacisuria and haematuria. After two months of therapy, intravesical tumour had disappeared at cystoscopy, but there was no response in the pelvic tumours or the lung metastases. At four months, radiotherapy of 50 Gy to the bladder and the prostate was given, but the bladder symptoms persisted. At six months, the lung metastases were progressing and the creatinine levels rose, indicating the need for nephrostomy for the right kidney. Because of poorly responding disease and nephrotoxic therapy, ISG/SSG IV protocol was changed to combined docetaxel and gemcitabine. During the new treatment, both the primary tumour and the metastases remained almost stable or showed only minor progression. The treatment was well tolerated and the general condition of the patient was good although there were repeated infections and occasional problems with nephrostomy catheter. The patient received 16 cycles of docetaxel-gemcitabine in total.

After 23 months of treatment, a subcutaneous metastasis was removed from the forehead. Lung metastases progressed and new metastases appeared in hilar and mediastinal lymph nodes and the right kidney. The patient also had intracerebral hemorrhage with right hemiparesis, from which he partially recovered. During his last month, the patient received palliative radiotherapy (30 Gy) of the mediastinum due to dyspnea and

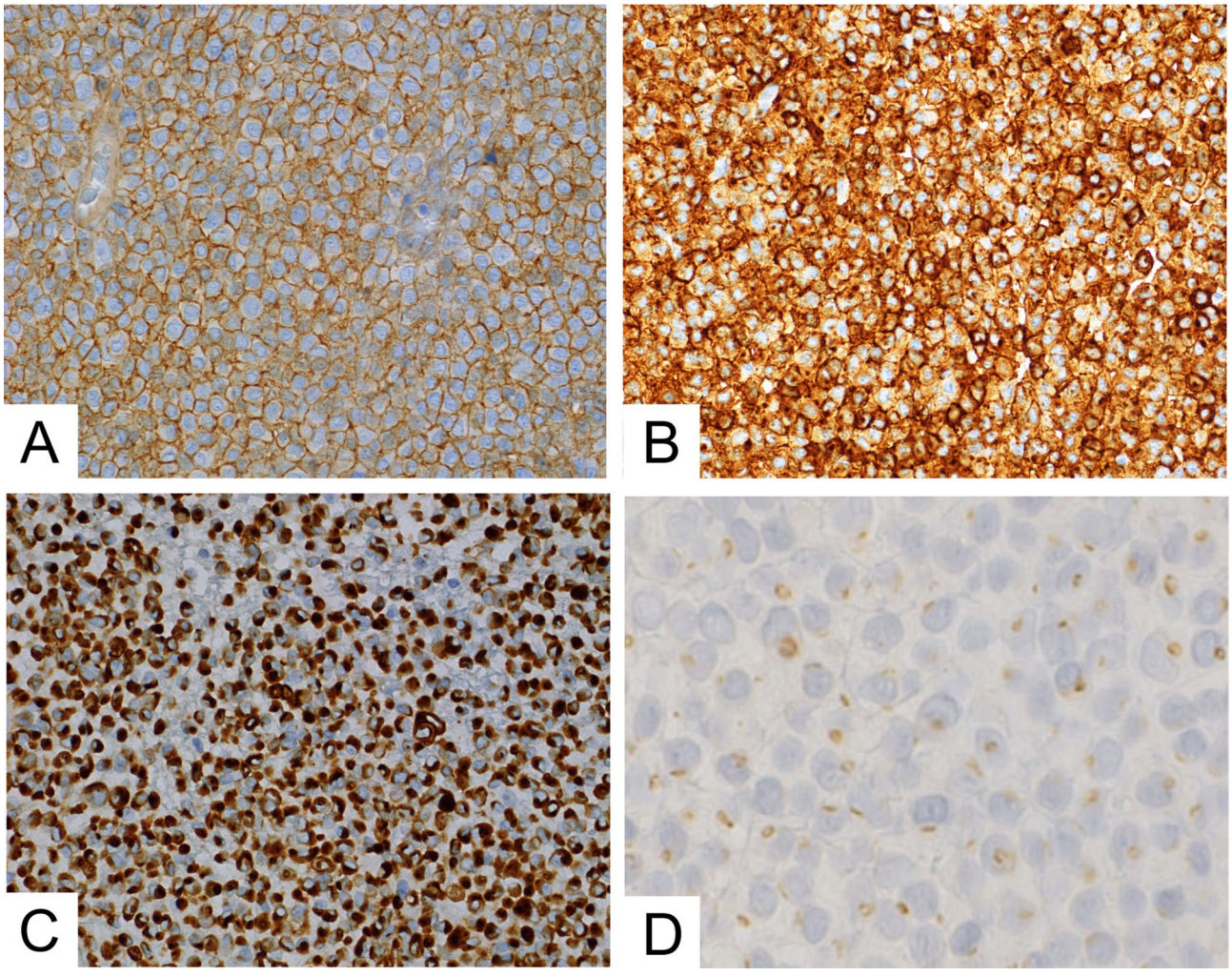

Fig. 3 Positive membranous staining for CD99 (**A**, 20 x) and EMA (**B**, 20x). Vimentin (**C**, 20x) and cytokeratin Cam 5.2 (**D**, 40x) with golgi-like perinuclear pattern

hemoptysis but his general condition deteriorated and further treatment was withdrawn. He died of the disease 26 months after the diagnosis at the age of 30 years 8 months.

At the time of diagnosis and treatment, tumor agnostic molecular techniques were not available as diagnostic tools. The tumor tissue was later studied with Illumina TruSight Pan-Cancer RNA sequencing panel and Infinium MethylationEPIC v2.0 kit as a part of a validation study. An in-frame fusion transcript with sequence from exon 10 of *EWSR1* gene (NM_005243.4, MANE Select transcript) attached to sequence from exon 2 of *BEND2* gene (NM_153346.5, MANE Select transcript) was observed (Fig. 4B). With the information provided by the bioinformatic pipeline, the contig sequence of the fusion site was confirmed with Sanger sequencing (Fig. 4B). The methylation profile of the tumor did not classify with the sarcoma classifier [2] (see Additional File 1) but the brain tumor classifier [3] suggested similarity to *MN1::BEND2* rearranged astroblastoma although with low prediction score (0.364). The copy number profile showed partial loss of chromosome areas 1q and 10q resulting in e.g. loss of tumor suppressor gene *PTEN* (Fig. 4C).

Discussion

We report an in-frame *EWSR1::BEND2* fusion in an undifferentiated small round cell sarcoma of the urinary bladder. In this rearrangement, the N-terminal transcription activation domain of *EWSR1* is fused to the C-terminal BEN domain of *BEN Domain Containing 2* (*BEND2*) gene. The same fusion has been described in a subset of astroblastoma, a glial tumor with perivascular rosette formation, where it replaces the more common *MN1* alterations [4–7]. Both structural elements of the fusion protein are also seen in the bladder tumor although the breakpoint of *EWSR1* differs from the breakpoints described in astroblastoma [7]. Outside central nervous system, verified *EWSR1::BEND2* fusions have been reported in

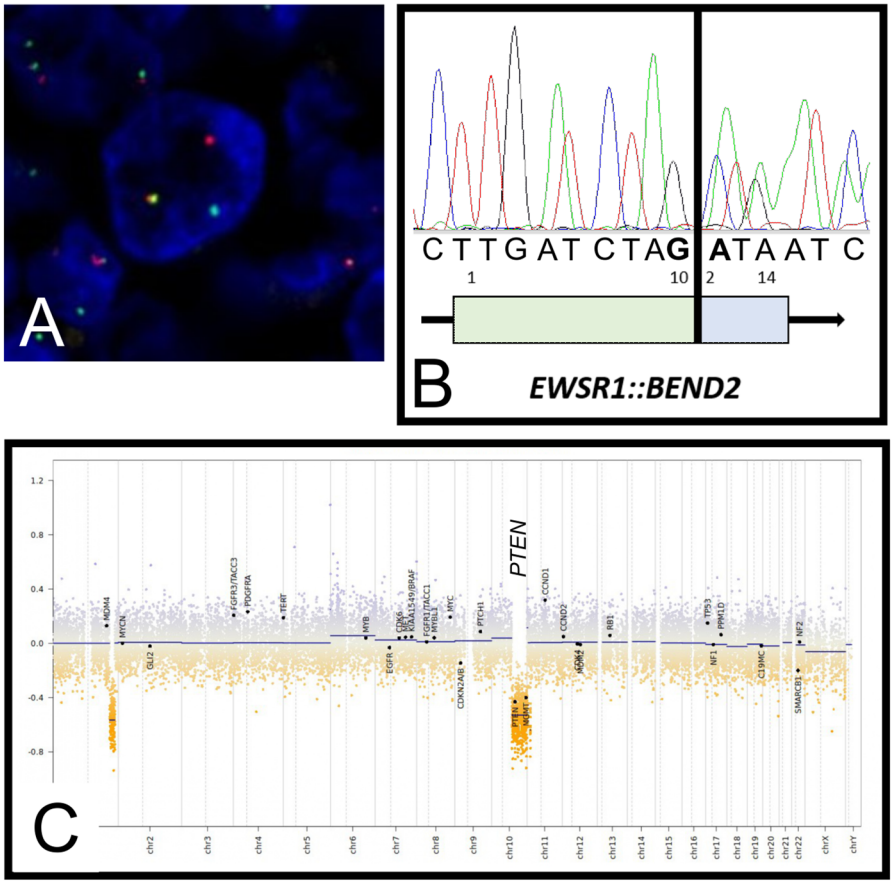

Fig. 4 Break-apart *EWSR1* fluorescence in situ hybridization showing translocation (**A**). Fusion transcript with sequence from exon 10 of *EWSR1* gene attached to sequence from exon 2 of *BEND2* gene along with confirmation of the fusion by Sanger sequencing (**B**). Copy number profile from methylation analysis showing partial loss of chromosome areas 1q and 10q, including tumor suppressor gene *PTEN* (**C**)

salivary gland carcinoma [8], adenocarcinoma of the trachea [9], neuroendocrine pancreatic tumor [10] and five cases (including the one described here) of mesenchymal tumors with differing morphologies, such as low-grade sinonasal sarcoma [11] and high-grade undifferentiated small cell and/or spindle cell neoplasms of bone [12, 13]. These tumors were cellular with round, epithelioid or spindle-shaped tumor cells. In immunohistochemistry showed diffuse or focal positivity for EMA (all cases) and cytokeratin (3 out of 5 cases). Although pseudorosette formation was also seen in an *EWSR1::BEND2* fused tracheal carcinoma, all the *BEND2* fused carcinomas have been reported to be strong cytokeratin positive [8, 9]. Our tumor had only weak golgi-like cytokeratin positivity which does not favor the diagnosis of a poorly differentiated carcinoma. Taken together, *EWSR1::BEND2* fusion is seen in a heterogeneous group of tumors with differing morphology. This highlights the biological heterogeneity of tumors with identical fusions, likely influenced by the cell of origin, epigenetic regulation, tumor microenvironment, and co-occurring genetic alterations [14].

EWSR1, coding for a transcription factor *EWS R*NA binding protein (EWSR1), is known to be rearranged in a variety of benign and malignant tumors with varying morphologies, the most common of these being Ewing Sarcoma (ES) [15]. The sole discovery of *EWSR1* translocation with fluorescence in situ hybridisation gives, thus, little information and should be used to confirm a working diagnosis [16, 17]. *EWSR1* is expressed in most cell types and plays its part in multiple physiological processes, such as organ development and aging through epigenetic regulation of gene transcription and RNA processing [18]. Therefore, *EWSR1* gene fusions can lead to complex transcriptional and phenotypic changes

when dysregulated in cancers [19]. Ewing sarcoma (ES), an undifferentiated small round cell sarcoma (USRCS) of soft tissue and bone, occurs mainly in children, adolescents and young adults [20]. The fusion gene behind ES, the most common being *EWSR1::FLI1* [20], involves one member of the FET family of genes, such as *EWSR1*, and a member of the ETS (erythroblast transformation specific) family of transcription factors. In addition to ES, the USRCS group consists of various malignancies that originate from bone and soft tissue: *CIC*-rearranged sarcoma, sarcoma with *BCOR* genetic alterations and round cell sarcoma with EWSR1-non-ETS fusions [20]. However, given the tumor agnostic approach of the modern molecular techniques, new previously undescribed tumor entities are being found continuously. By definition *EWSR1::BEND2* rearranged small round cell sarcoma could classify in the EWSR1-non-ETS Fusion sarcoma group in the latest WHO classification [20]. The group consists of exceedingly rare round and spindle cell sarcomas with *EWSR1* or *FUS* fusions involving fusion partners other than the ETS gene family. The most common of these fusions appears to be *EWSR1::NFATC2*, which causes sarcomas usually located in bones more often than soft tissue, with a ratio of 4:1 [21]. It is usually located in the metaphysis or diaphysis of long bones such as the femur, humerus, radius and tibia. Another fusion in this group is the *EWSR1::PATZ1* fusion. *NFATC2* encodes a transcription factor, which plays a role in T-cell differentiation and the activation of cytokines, whereas *PATZ1* is responsible for encoding a zinc finger protein with tumor suppressive functions [22–25]. Similar to the group of *BEND2* rearranged EWSR1-non-ETS sarcomas, a newly characterized group of *EWSR1::POU2AF3* has been expanding [26–28] and to date 21 cases with polyphenotypic sarcomatous morphology and predilection to sinonasal area have been characterised. The group of EWSR1-non-ETS Fusions is evolving due to discovery of new fusions, such as *EWSR1::BEND2* or *EWSR1::POU2AF3*, and this may lead to the need for reorganizing this category in the future editions of the WHO classification.

From a therapeutic standpoint, given the rarity and heterogeneity of the tumors, genetic testing may also reveal co-occurring alterations with clinical relevance. A broad genetic test can give additional information guiding the treatment towards gene alteration, such as *PTEN* loss seen here. Phosphatase and tensin homologue *PTEN*, one of the most commonly somatically mutated or deleted genes in cancer, is a tumor suppressor gene affecting the PI3K/AKT/mTOR pathway [29]. *PTEN* loss may affect the efficacy of immune-oncological treatments [30] but there is evidence that patients with defective *PTEN* might benefit from mTOR inhibitors [31] or PARP inhibitors [32]. Therefore, although genome-wide testing is not mandatory, our example highlights the potential value of molecular findings in treatment planning, even when the targetable mutations are not the primary driver.

As a conclusion, we report an undifferentiated small round cell sarcoma of the bladder harbouring *EWSR1::BEND2* fusion. As tumor agnostic genomic approach is used more widely, new tumor entities with tumor defining genomic alterations are found increasingly. According to ESMO Guidelines, ES-like approach has usually been chosen for treatment of these new entities [33]. It is, however, important that the treatment in these cases follows established treatment protocols so that information for the clinical behaviour of these ultra-rare sarcomas can be documented.

Supplementary Information

The online version contains supplementary material available at https://doi.org/10.1186/s13000-025-01721-3.

Additional file 1. The UMAP model was generated using 27,543 cases with a high sarcoma v13 classifier score (>0.7). Our tumor is located in a region between cases predominantly assigned to the subclasses epithelioid sarcoma (ES), cutaneous squamous cell carcinoma (SCC), and poorly differentiated chordoma (CHORD_POD) but does not appear to resemble any subclass included in the training of the sarcoma classifier.

Acknowledgements
We want to acknowledge Dr Martin Sill (Heidelberg Epignostix GmbH) for the help with methylation data and the UMAP generation.

Authors' contributions
VH and KO wrote the manuscript. JT and KO did the genomic work (RNA sequencing) and Methylome analysis. MK collected the material and made the preliminary diagnosis, MK and KO further analysed the case later when new information (RNA sequencing and new WHO classification) were available. PL together with VH collected the information concerning the treatment of the patient and commented on the manuscript concerning this data. TK was the radiologist responsible for the preliminary imaging analysis and further with VH analysed the collected imaging data for the manuscript and commented on the manuscript written by VH. All co-authors commented on the manuscript and approved the last version.

Data availability
No datasets were generated or analysed during the current study.

Declarations

Competing interests
The authors declare no competing interests.

Received: 22 June 2025 / Accepted: 21 September 2025
Published online: 16 October 2025

References

1. Luksch R, et al. Primary metastatic Ewing's family tumors: results of the Italian Sarcoma Group and Scandinavian Sarcoma Group ISG/SSG IV study including myeloablative chemotherapy and total-lung irradiation. Ann Oncol. 2012;23(11):2970–6. https://doi.org/10.1093/annonc/mds117.
2. Koelsche C, et al. Sarcoma classification by DNA methylation profiling. Nat Commun. 2021;12(1):498. https://doi.org/10.1038/s41467-020-20603-4.

3. Capper D, et al. DNA methylation-based classification of central nervous system tumours. Nature. 2018;555(7697):469–74. https://doi.org/10.1038/nature26000.
4. Smith-Cohn MA, et al. Molecular clarification of brainstem astroblastoma with EWSR1-BEND2 fusion in a 38-year-old man. Free Neuropathol. Jan. 2021;2:16. https://doi.org/10.17879/freeneuropathology-2021-3334.
5. Tsutsui T, et al. Spinal cord astroblastoma with EWSR1-BEND2 fusion classified as HGNET-MN1 by methylation classification: a case report. Brain Tumor Pathol. 2021;38(4):283–9. https://doi.org/10.1007/s10014-021-00412-3.
6. Yamasaki K, et al. Spinal cord astroblastoma with an EWSR1-BEND2 fusion classified as a high-grade neuroepithelial tumour with MN1 alteration. Neuropathol Appl Neurobiol. 2020;46(2):190–3. https://doi.org/10.1111/nan.12593.
7. Lucas C-HG, et al. EWSR1-BEND2 fusion defines an epigenetically distinct subtype of astroblastoma. Acta Neuropathol. 2022;143(1):109–13. https://doi.org/10.1007/s00401-021-02388-y.
8. Zhang Y-D, et al. Malignant salivary gland neoplasm of the tongue base with EWSR1::BEND2 fusion: an unusual case with literature review. Head Neck Pathol. 2024;18(1):118. https://doi.org/10.1007/s12105-024-01726-2.
9. Sanchez-Ramirez JJ, Hoffman MR, Keech JC, Snow AN, Bellizzi AM, Rajan A. EWSR1::BEND2 adenocarcinoma with hyaline pseudorosettes of the trachea. Head Neck Pathol. 2025;19(1):7. https://doi.org/10.1007/s12105-024-01746-y.
10. Scarpa A, et al. Whole-genome landscape of pancreatic neuroendocrine tumours. Nature. 2017;543(7643):65–71. https://doi.org/10.1038/nature21063.
11. Palsgrove DN, Manucha V, Park JY, Bishop JA. A low-grade sinonasal sarcoma harboring EWSR1::BEND2: expanding the differential diagnosis of sinonasal spindle cell neoplasms. Head Neck Pathol. 2023;17(2):571–5. https://doi.org/10.1007/s12105-023-01527-z.
12. Salguero-Aranda C, et al. Identification of novel/rare EWSR1 fusion partners in undifferentiated mesenchymal neoplasms. Int J Mol Sci. 2024;25(3):1735. https://doi.org/10.3390/ijms25031735.
13. Çetin S, et al. EWSR1::BEND2 fusion sarcoma in bone: a report of two rare cases. Virchows Arch. 2025;486(4):877–85. https://doi.org/10.1007/s00428-025-04063-z.
14. Tuna M, Amos CI, Mills GB. Molecular mechanisms and pathobiology of oncogenic fusion transcripts in epithelial tumors. Oncotarget. 2019;10:2095–111. https://doi.org/10.18632/oncotarget.26777.
15. Jedlicka P. Ewing sarcoma, an enigmatic malignancy of likely progenitor cell origin, driven by transcription factor oncogenic fusions. Int J Clin Exp Pathol. 2010;3(4):338–47.
16. Walker V, et al. Gene partners of the EWSR1 fusion may represent molecularly distinct entities. Transl Oncol. 2023;38:101795. https://doi.org/10.1016/j.tranon.2023.101795.
17. Towery EA, Papke DJ. EWSR1: the promiscuous king of mesenchymal neoplasia. J Clin Pathol. 2024;77(11):721–5. https://doi.org/10.1136/jcp-2023-208867.
18. Lee J, et al. EWSR1, a multifunctional protein, regulates cellular function and aging via genetic and epigenetic pathways. Biochimica et Biophysica Acta (BBA). 2019;1865:1938–45. https://doi.org/10.1016/j.bbadis.2018.10.042.
19. Flucke U, et al. EWSR1-the most common rearranged gene in soft tissue lesions, which also occurs in different bone lesions: an updated review. Diagnostics. 2021;11(6):1093. https://doi.org/10.3390/diagnostics11061093.
20. Organisation mondiale de la santé and Centre international de recherche sur le cancer. Eds., *Soft tissue and bone tumours*, 5th ed. in World health organization classification of tumours, no. Vol. 3. Geneva: OMS, 2020.
21. Diaz-Perez JA, Nielsen GP, Antonescu C, Taylor MS, Lozano-Calderon SA, Rosenberg AE. EWSR1/FUS-NFATc2 rearranged round cell sarcoma: clinicopathological series of 4 cases and literature review. Hum Pathol. 2019;90:45–53. https://doi.org/10.1016/j.humpath.2019.05.001.
22. Fedele M, Crescenzi E, Cerchia L. The POZ/BTB and AT-hook containing zinc finger 1 (PATZ1) transcription regulator: physiological functions and disease involvement. Int J Mol Sci. 2017;18(12):2524. https://doi.org/10.3390/ijms18122524.
23. Mastrangelo T. A novel zinc finger gene is fused to EWS in small round cell tumor. Oncogene. 2000;19(33):3799–804. https://doi.org/10.1038/sj.onc.1203762.
24. Machado I, et al. Sarcomas with EWSR1::Non-ETS fusion (EWSR1::NFATC2 and EWSR1::PATZ1). Surg Pathol Clin. 2024;17(1):31–55. https://doi.org/10.1016/j.path.2023.07.001.
25. Cohen JN, Sabnis AJ, Krings G, Cho S-J, Horvai AE, Davis JL. EWSR1-NFATC2 gene fusion in a soft tissue tumor with epithelioid round cell morphology and abundant stroma: a case report and review of the literature. Hum Pathol. 2018;81:281–90. https://doi.org/10.1016/j.humpath.2018.03.020.
26. Hiemenz MC, et al. POU2AF3-rearranged sarcomas: a novel tumor defined by fusions of EWSR1 or FUS to a gene formerly designated COLCA2. Genes Chromosomes Cancer. 2023;62(8):460–70. https://doi.org/10.1002/gcc.23136.
27. Çetin S, Yılmaz İ, Bakkaloğlu DV, Çelik M, Bilgiç B, Özlük Y. Sinonasal *EWSR1::POU2AF3* sarcoma: a case report and literature review. Virchows Arch Int J Pathol. 2025;486(4):855–64. https://doi.org/10.1007/s00428-025-04055-z.
28. Koshyk O, et al. EWSR1::POU2AF3(COLCA2) sarcoma: an aggressive, polyphenotypic sarcoma with a head and neck predilection. Mod Pathol. 2023;36(12):100337. https://doi.org/10.1016/j.modpat.2023.100337.
29. Lee Y-R, Chen M, Pandolfi PP. The functions and regulation of the PTEN tumour suppressor: new modes and prospects. Nat Rev Mol Cell Biol. 2018;19(9):547–62. https://doi.org/10.1038/s41580-018-0015-0.
30. Vidotto T, Melo CM, Castelli E, Koti M, Dos RB, Reis, Squire JA. Emerging role of PTEN loss in evasion of the immune response to tumours, *Br. J. Cancer*, vol. 122, no. 12, pp. 1732–1743, Jun. 2020, https://doi.org/10.1038/s41416-020-0834-6
31. Weeber F, et al. Predicting clinical benefit from everolimus in patients with advanced solid tumors, the CPCT-03 study. Oncotarget. 2017;8(33):55582–92. https://doi.org/10.18632/oncotarget.16029.
32. Mendes-Pereira AM, et al. Synthetic lethal targeting of PTEN mutant cells with PARP inhibitors. EMBO Mol Med. 2009;1(6–7):315–22. https://doi.org/10.1002/emmm.200900041.
33. Strauss SJ et al. Dec., Bone sarcomas: ESMO-EURACAN-GENTURIS-ERN PaedCan Clinical Practice Guideline for diagnosis, treatment and follow-up, *Ann. Oncol. Off. J. Eur. Soc. Med. Oncol.*, vol. 32, no. 12, pp. 1520–1536, 2021, https://doi.org/10.1016/j.annonc.2021.08.1995

Publisher's Note